Thermally induced birefringence in Faraday devices made from terbium gallium garnet–polycrystalline ceramics

Mikhail A. Kagan and Efim A. Khazanov

We have developed a model that describes thermally induced birefringence in polycrystalline ceramics that are exposed to a magnetic field. Conditions under which traditional compensation techniques (for glass and single crystals) can be effective for ceramics have been found. It is shown that a ceramic is almost equivalent to a [111]-oriented crystal if the ratio of the rod length to the grain size is ~300 or more. In particular, residual depolarization (after the compensation techniques are applied) is inversely proportional to this ratio, which is an important consequence of the random nature of thermally induced birefringence in ceramics. © 2004 Optical Society of America

OCIS codes: 190.4870, 160.3820, 230.3240.

1. Introduction

Recently polycrystalline Nd:YAG ceramics used as laser-active elements have attracted much attention because they have several essential advantages compared with Nd:YAG single crystals.[1–12] Modern technology allows for producing active elements of good optical quality, large aperture, and high concentrations of Nd ions. Many properties of ceramics are similar to those of single crystals. However, thermally induced depolarization of radiation exhibits some differences.[6–9]

Polycrystalline ceramics can be used not only as active media and Q switches[13] but for construction of Faraday isolators and Faraday mirrors based on magnetoactive elements made from terbium gallium garnet (TGG) as well. There are no serious difficulties in TGG–ceramic production, and the first TGG samples (not of high quality, though) have already been produced.[14] The Faraday isolator and Faraday mirror are drastically affected by thermal self-action caused by the relatively high (compared with that of quartz or glass) radiation absorption in magnetoactive media, $\sim 10^{-3}$ cm^{-1} or greater. In magnetoactive Faraday elements (FEs) the photoelastic effect leads to parasitic linear birefringence imposed on useful circular birefringence (the Faraday effect).[15,16]

Polycrystalline ceramics consist of a number of single crystal grains separated by thin boundaries. The essential difference between ceramics and single crystals is that the crystal axes in each grain that composes ceramics are arbitrarily oriented. As distinct from a single crystal, ceramics constitute a set of elliptic phase plates with arbitrary orientations of eigenpolarizations and the phase delay between them.

A model of thermally induced birefringence in polycrystalline ceramics without a magnetic field was introduced in Refs. 7–9. In the present paper we generalize this model to the case of ceramic samples exposed to a magnetic field and derive analytical expressions for the depolarization of radiation in FEs, and we investigate the effectiveness of compensation for the depolarization by means of all known techniques for single crystals or glass. We applied the quaternion formalism[17] (instead of the traditional Jones matrix formalism) to describe the depolarization of a laser beam. The analytic results that we obtained are in good agreement with numerical calculations.

2. Depolarization of Radiation in Ceramic Faraday Elements

A. Polarization Properties of Magnetoactive Ceramic Elements

Consider a transversely polarized laser beam incident upon an optical element. Denote by $\mathbf{e}_0$ and $\mathbf{e}$ the initial and the final (after the beam has passed through the element) polarizations, respectively.

M. A. Kagan is with the Davey Laboratory, Department of Physics, Pennsylvania State University, University Park, Pennsylvania 16802. E. A. Khazanov (khazanov@appl.sci-nnov.ru) is with the Institute of Applied Physics, 46 Uljanov Street, Nizhny Novgorod, 603950 Russia.

Received 13 January 2004; revised manuscript received 20 August 2004; accepted 26 August 2004.

0003-6935/04/326030-10$15.00/0

The relationship between $\mathbf{e}_0$ and $\mathbf{e}$ is conventionally expressed in terms of a 2×2 Jones matrix, $\mathbf{U}$:

$$\mathbf{e} = \mathbf{U}\mathbf{e}_0 (|\mathbf{e}| = |\mathbf{e}_0| = 1). \tag{1}$$

We define a local depolarization ratio Γ as the fraction of transmitted energy contained in polarization $\mathbf{e}_\perp$ orthogonal to $\mathbf{e}_0$:

$$\Gamma = |\mathbf{e}_\perp{}^* \mathbf{e}|^2 = \mathbf{e}_0{}^* \mathbf{U}^* \mathbf{e}_\perp \mathbf{e}_\perp{}^* \mathbf{U} \mathbf{e}_0. \tag{2}$$

Here and in what follows, an asterisk denotes Hermitian conjugation. Note that the components of $\mathbf{U}$ are written in some reference frame (x, y) (z is aligned with the wave vector). Below, we make extensive use of Eq. (2) for an incident polarization that forms angle $-\varphi$ with the x axis:

$$\begin{aligned} \mathbf{e}_0 &= \begin{bmatrix} \cos\varphi \\ -\sin\varphi \end{bmatrix}, \\ \mathbf{e}_0{}^* &= [\cos\varphi, -\sin\varphi], \\ \mathbf{e}_\perp &= \begin{bmatrix} \sin\varphi \\ \cos\varphi \end{bmatrix}, \\ \mathbf{e}_\perp{}^* &= [\sin\varphi, \cos\varphi]. \end{aligned} \tag{3}$$

Equation (2) becomes

$$\Gamma = \mathbf{e}_0{}^* \mathbf{G} \mathbf{e}_0,$$

where

$$\begin{aligned} \mathbf{G} &= \mathbf{U}^* \mathbf{M} \mathbf{U}, \qquad \mathbf{M} = \mathbf{e}_\perp \otimes \mathbf{e}_\perp{}^* \\ &= \begin{bmatrix} \sin^2\varphi & \sin\varphi\cos\varphi \\ \sin\varphi\cos\varphi & \cos^2\varphi \end{bmatrix}. \end{aligned} \tag{4}$$

Given the presence of induced linear birefringence, a FE (a single crystal or a grain) is described by the Jones matrix[18,19]

$$\mathbf{U} = \mathbf{Q}(\delta_l, \delta_c, \theta) = \begin{bmatrix} \cos\frac{\delta}{2} + i\frac{\delta_l}{\delta}\sin\frac{\delta}{2}\cos 2\theta & -\frac{\delta_c}{\delta}\sin\frac{\delta}{2} - i\frac{\delta_l}{\delta}\sin\frac{\delta}{2}\sin 2\theta \\ \frac{\delta_c}{\delta}\sin\frac{\delta}{2} - i\frac{\delta_l}{\delta}\sin\frac{\delta}{2}\sin 2\theta & \cos\frac{\delta}{2} - i\frac{\delta_l}{\delta}\sin\frac{\delta}{2}\cos 2\theta \end{bmatrix}, \tag{5}$$

where

$$\delta^2 = \delta_l{}^2 + \delta_c{}^2,$$

and where δ_c and δ_l are phase delays for purely circular (without linear) and for purely linear (without circular) birefringence, respectively, and θ is the angle of inclination of the purely linear eigenpolarization to the x axis. Note that the angle of rotation of the polarization plane is $\delta_c/2$. The direction of rotation is defined by the sign of δ_c, so a positive δ_c refers to counterclockwise rotation. Note, in particular, that matrix $\mathbf{Q}(0, \delta_c, 0)$ describes a rotator that produces rotation by angle $\delta_c/2$, whereas $\mathbf{Q}(\delta_l, 0, \theta)$ corresponds to a linear phase plate with phase delay δ_l and inclination of eigenpolarization θ. In what follows, we use the notation $\mathbf{Q}$ not only for ceramic samples but also for some other optical elements.

Consequently, Jones matrix $\mathbf{T}$ that describes a ceramic sample is the product of N matrices (N is the number of grains through which the laser beam passes):

$$\mathbf{T} = \mathbf{Q}_N \mathbf{Q}_{N-1} \ldots \mathbf{Q}_2 \mathbf{Q}_1. \tag{6}$$

Here the subscript k labels the grains, and matrix $\mathbf{Q}_k = \mathbf{Q}(\delta_{lk}, \delta_{ck}, \theta_k)$ depends on the corresponding δ and θ, which are random variables.

Although the depolarization ratio in ceramics is a statistical variable, it is natural to characterize the polarization properties of a ceramic sample by certain average quantities. We denote by $\langle \mathbf{G} \rangle$ the matrix $\mathbf{G}$ averaged over the beam path, and we write the mean depolarization as

$$\langle \Gamma \rangle = \mathbf{e}_0{}^* \langle \mathbf{G} \rangle \mathbf{e}_0. \tag{7}$$

B. Compensation of Depolarization in Faraday Elements

Besides the traditional designs of the Faraday isolator [Fig. 1(a)] and of the Faraday mirror [Fig. 1(e)], designs with compensation for (thermally induced) parasitic birefringence [Figs. 1(b)–1(d) and 1(f)] are used.[15,20–23] The physical reason for the depolarization reduction in the new designs of the Faraday isolator is the fact that the polarization distortions that the beam suffers in propagating through the first FE are compensated for when the beam propagates through the second FE [Figs. 1(b) and 1(c)] or the uniaxial crystal [Fig. 1(d)]. The polarization distortions that the beam suffers in propagating through the new Faraday mirror design [Fig. 1(f)] are compensated for in backward propagation. The depolarization for each design is calculated according to Eq. (7). The only difference is in the $\mathbf{U}$ and $\mathbf{G}$ matrices that describe a particular optical system. As was mentioned above, the Jones matrix of a ceramic element $\mathbf{T}$ is a product of matrices for individual grains [Eq. (6)]. Thus the $\mathbf{G}$ matrix for an uncompensated Faraday isolator [Fig. 1(a)] is given by

$$\begin{aligned} \mathbf{G_a} &= \mathbf{T}^* \mathbf{M} \mathbf{T} \\ &= \mathbf{Q}_1{}^* \mathbf{Q}_2{}^* \ldots \mathbf{Q}_{N-1}{}^* \mathbf{Q}_N{}^* \mathbf{M} \mathbf{Q}_N \mathbf{Q}_{N-1} \ldots \mathbf{Q}_2 \mathbf{Q}_1. \end{aligned} \tag{8}$$

Denoting by Δ_l and Δ_c the total linear and circular phase delays, respectively, in a ceramic element, we

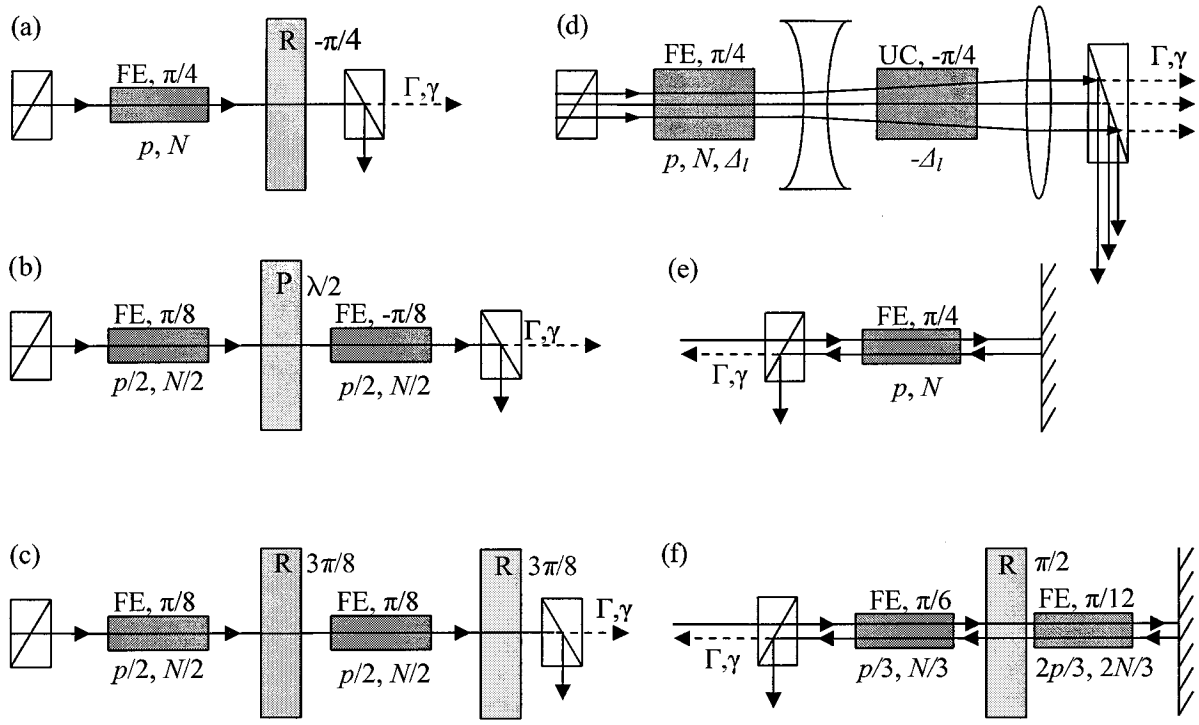

Fig. 1. Designs of Faraday isolators: (a) without compensation; (b) with a half-wave plate (P) (Refs. 15 and 20); (c) with reciprocal rotator (R) by $3\pi/8$ (Refs. 15 and 20); and (d) with a uniaxial crystal (UC) (Ref. 21). Designs of Faraday mirrors: (e) without compensation and (f) with a reciprocal rotator (R) by $\pi/2$.[22,23] Angles above the Faraday elements indicate the angles of polarization-plane rotation. p and N stand for power and number of grains, respectively, for the entire beam path.

write a **U** matrix that corresponds to each design. In Fig. 1(a),

$$\mathbf{U_a} = \mathbf{Q}(0, -\pi/2, 0)\mathbf{T}(\Delta_c = \pi/2). \tag{8a}$$

The axis of the half-wave plate [Fig. 1(b)] is inclined to the x' axis by $\pi/8$. Thus the plate is described by matrix $\mathbf{Q}(\pi, 0, \pi/8 - \phi)$, and **U** takes the form

$$\mathbf{U_b} = \mathbf{T}_2(\Delta_c = -\pi/4)\mathbf{Q}(\pi, 0, \pi/8 - \phi)\mathbf{T}_1(\Delta_c = \pi/4). \tag{8b}$$

In the design of Fig. 1(c),

$$\mathbf{U_c} = \mathbf{Q}(0, 3\pi/4, 0)\mathbf{T}_2(\Delta_c = \pi/4) \times \mathbf{Q}(0, 3\pi/4, 0)\mathbf{T}_1(\Delta_c = \pi/4). \tag{8c}$$

The telescope in Fig. 1(d) has the matrix $\mathbf{Q}(-\Delta_l, -\Delta_c, 0)$ corresponding to it. Accordingly,

$$\mathbf{U_d} = \mathbf{Q}(-\Delta_l, -\Delta_c, 0)\mathbf{T}(\Delta_c = \pi/2). \tag{8d}$$

The Faraday mirror in Fig. 1(e) rotates the initial polarization by $\pi/2$. To calculate only the additional rotation that is due to depolarization, to be consistent with the definition of Eq. (2) we account for this Faraday rotation by multiplying the Jones matrix by $\mathbf{Q}(0, \pi, 0)$, which refers to a rotation by $\pi/2$. Hence

$$\mathbf{U_e} = \mathbf{T}(\Delta_c = \pi)\mathbf{Q}(0, \pi, 0). \tag{8e}$$

In the same fashion we assume an auxiliary rotation by $-\pi/2$ in the last design. Note also that we treat the leftmost FE as two different elements when the laser beam goes to the right ($\mathbf{T}_1$) or to the left ($\mathbf{T}_3$). $\mathbf{T}_2$ refers to a right FE:

$$\begin{aligned}\mathbf{U_f} &= \mathbf{Q}(0, \pi, 0)\mathbf{T}_3(\Delta_c = \pi/6)\mathbf{Q}(0, \pi, 0)\mathbf{T}_2(\Delta_c = \pi/6)\mathbf{Q}(0, -\pi, 0)\mathbf{T}_1(\Delta_c = \pi/4) \\ &\equiv \mathbf{Q}(0, \pi, 0)\mathbf{T}_3(\Delta_c = \pi/6)\mathbf{T}_2{}^*(\Delta_c = -\pi/6)\mathbf{T}_1(\Delta_c = \pi/4).\end{aligned} \tag{8f}$$

The corresponding **G** matrices are related to the **U** matrices above through Eq. (4).

To evaluate $\langle\Gamma\rangle$ by using Eqs. (7) and (8), one needs to know the distribution function that depends on all the values of δ and φ. Determining this function is a quite complicated task, insofar as the prescribed quantities depend on the mutual positioning of crystal axes in each grain and on the direction of the temperature gradient. Such dependence for a single crystal was derived in Ref. 7 and is introduced in

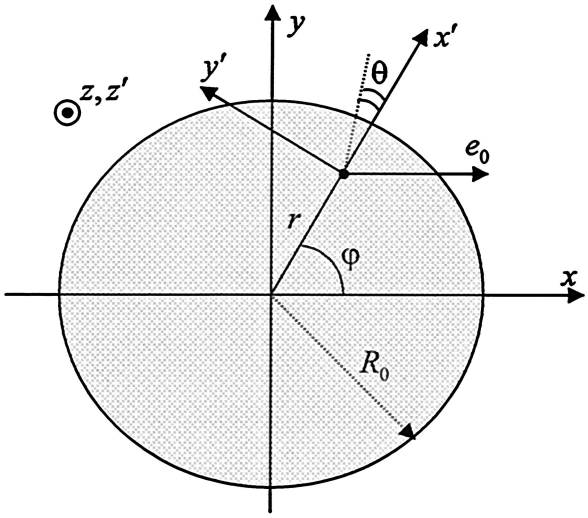

Fig. 2. Coordinate frames xyz and $x'y'z'$.

Section 3 of the present paper, where we apply these results to ceramic active elements.

3. Eigenpolarization in a Single Crystal and Ceramics

Radiation absorption in magnetoactive media is a source of heat generation that leads to polarization distortions in Faraday devices. In this section, eigenpolarizations should be thought of as eigenpolarizations for single ceramic grains. At the end of this paper we discuss the possibility of a sensible notion of eigenpolarizations for the entire ceramic sample.

Consider a cylindrical sample of radius R_0 and length L. We apply the geometrical optics approach and assume that the laser beam is a set of rays parallel to the sample's axis of symmetry z. One of those rays is introduced in Fig. 2. It is marked by r, the distance between the beam and the rod axis, and ϕ, the azimuthal angle. We also assume that the incident wave is linearly polarized along the x axis such that its polarization in the primed reference frame (Fig. 2) has the form prescribed in Eqs. (3). In what follows, all Jones matrices are also written on the primed basis.

Let the heat-release power density in the FE be independent of z and ϕ. This is reasonable if the laser beam is axially symmetric and the power absorbed over the whole length of the FE is much smaller than the laser power. Consequently, the temperature gradient possesses radial symmetry and induces in each cross section two preferential directions: radial and azimuthal (x' and y' in Fig. 2). The polarization properties of the sample depend on the temperature distribution and on the positioning of crystallographic axes abc with respect to reference system xyz.[7,24] In the trivial case the abc axes coincide with the xyz directions, which correspond to the [001] orientation. An arbitrary positioning of the abc axes is produced by three sequential rotations of the xyz coordinate system relative to the crystal lattice. These rotations are labeled with Euler angles α, β, and Φ.[25] The reference system is rotated first by angle α ($\alpha \in [-\pi, \pi]$) about the z-axis aligned with crystal axis c; then by angle β ($\beta \in [-\pi/2, \pi/2]$) about the y axis; and, finally, about the z axis by angle Φ ($\Phi \in [-\pi, \pi]$). The third rotation does not affect the mutual orientation of the sample axis and the z direction. We emphasize that for a single crystal it does not cause any physically important changes, as this rotation is equivalent to a different choice of the coordinate system, rotated about the z axis by angle Φ. In other words, one is always able to choose a reference frame in which $\Phi = 0$ and the z direction is aligned with the wave vector of the laser beam. Nevertheless, the last-named rotation turns out to be essential when one is dealing with ceramics. Angle Φ is different for different ceramic grains, and there is no coordinate system that yields a zero value for Φ in every grain. Thus the orientation of crystallographic axes abc in a given grain is determined by three Euler angles, α, β, and Φ, which are random variables distributed uniformly within their respective intervals.

Using the equations in Ref. 7, we can express the relationship between the Euler angles of a certain grain and the quantities θ (measured from the x' axis in Fig. 2) and δ as follows:

$$\tan 2\theta = \tilde{b}/\tilde{a}, \qquad \delta = -\frac{p}{N}\frac{l_g}{\langle l_g \rangle}\frac{\tilde{a}}{\cos 2\theta}, \tag{9}$$

where

$$\begin{aligned}
\tilde{a} &= \xi h + \frac{\xi - 1}{8}(g\sigma_1 + h\tau_1),\\
\tilde{b} &= \frac{\xi - 1}{8}(g\sigma_2 + h\tau_2),\\
\sigma_1 &= \sin^2\beta\{[8\cos^2\beta - \sin^2 2\alpha(3 + \cos 2\beta)]\cos 2\Phi'\\
&\quad + 2\cos\beta \sin 4\alpha \sin 2\Phi'\},\\
\sigma_2 &= \sin^2\beta\{[8\cos^2\beta - \sin^2 2\alpha(3 + \cos 2\beta)]\sin 2\Phi'\\
&\quad - 2\cos\beta \sin 4\alpha \cos 2\Phi'\},\\
\tau_1 &= -4\cos^2\beta - \sin^4\beta(4 - \sin^2\alpha)\\
&\quad - \cos 4\Phi'[\sin^4\beta(4 - \sin^2 2\alpha)\\
&\quad + 4\cos^2\beta \cos 4\alpha] - \sin 4\Phi'\\
&\quad \times \sin 4\alpha \cos\beta(3 + \cos 2\beta),\\
\tau_2 &= \sin 4\alpha \cos\beta(3 + \cos 2\beta)\cos 4\Phi'\\
&\quad - [\sin^4\beta(4 - \sin^2 2\alpha) + 4\cos^2\beta \cos 4\alpha]\\
&\quad \times \sin 4\Phi',\\
p &= \frac{P_h}{\lambda}\frac{a_T}{\kappa}\frac{n_0^3}{4}\frac{1 + \nu}{1 - \nu}(p_{11} - p_{12}),\\
\xi &= \frac{2p_{44}}{p_{11} - p_{12}},\\
\Phi' &= \Phi - \varphi.
\end{aligned} \tag{10}$$

Here P_h is the heat-release power deposited in all FEs, λ is the wavelength, κ is the coefficient of thermal conductivity, α_T is the thermal expansion coefficient, n_0 is the index of refraction without heating, ν is the Poisson coefficient, p_{ij} are the photoelastic coefficients, and l_g is the grain size (a normally distributed random variable with mean value $\langle l_g \rangle$ and root-mean-square deviation σ_l). For any fixed Euler angles Eqs. (9) and (10) yield θ and δ for a single crystal of corresponding orientation. For instance, setting $\alpha = \beta = \Phi = 0$ ([001] orientation) or $\alpha = \pi/4$, $\tan\beta = \sqrt{2}$, and $\Phi =$ any angle ([111] orientation), one gets the well-known[26,27] expressions $\tan(2\theta + 2\varphi) = \xi \tan(2\varphi)$ and $\theta = 0$, respectively. Note that, as Φ is a random variable distributed uniformly within the interval $[-\pi, \pi]$, the prime on Φ in the expressions for $\sigma_{1,2}$ and $\tau_{1,2}$ can be omitted when one is averaging over Φ'.

The functions g and h are expressed by means of form factor f of the laser beam's intensity $I = I_0 f(r^2/{r_0}^2)$ according to[7]

$$h(u) = \frac{1}{u}\int_0^u \mathrm{d}z \int_0^z f(x)\mathrm{d}x,$$

$$g(u) = \frac{1}{R}\int_0^R \mathrm{d}z \int_0^z f(x)\mathrm{d}x - \int_u^R \frac{\mathrm{d}z}{z}\int_0^z f(x)\mathrm{d}x, \quad (11)$$

where $u = (r/r_0)^2$ and r_0 is the radius of the beam.

In particular, for a flat-shaped beam

$$f = \Theta(1-u), \qquad h = u/2, \qquad g = u - 1/2, \quad (11a)$$

and for a Gaussian beam

$$f = \exp(-u),$$

$$h = 1 + \frac{\exp(-u) - 1}{u},$$

$$g = 1 + \frac{\exp(-R) - 1}{R} + \ln\left(\frac{u}{R}\right) + \mathrm{Ei}(u) - \mathrm{Ei}(R), \quad (11b)$$

where $\Theta(x)$ is the unit function, $\mathrm{Ei}(x) = \int_1^\infty [\exp(-xt)/t]\,\mathrm{d}t$, and $R = (R_0/r_0)^2$. Note that the quantity ξ is a constant that characterizes a given crystal. In TGG, for instance, $\xi = 2.25$.[24,28] Note that Eqs. (9) and (10) yield a zero value for $\langle\theta\rangle$ when it is averaged over α, β, and Φ.

As the $\mathbf{T}$ matrix of the ceramic sample depends on r and φ, so does depolarization ratio Γ. We call the local depolarization $\Gamma(r, \varphi)$. Integral (average over the cross section of the rod) depolarization γ is also of interest:

$$\gamma = \frac{1}{\pi {R_0}^2}\int_0^{2\pi} \mathrm{d}\varphi \int_0^{R_0} \langle\Gamma\rangle(r, \varphi) f\left(\frac{r^2}{{r_0}^2}\right) r\mathrm{d}r$$

$$= \frac{1}{2\pi}\int_0^{2\pi} \mathrm{d}\varphi \int_0^1 \langle\Gamma\rangle(u, \varphi) f(u)\mathrm{d}u. \quad (12)$$

4. Mathematical Statement of the Problem and Solution

In this section we introduce the model optical system that describes the ceramic elements. To simplify the problem, we have made the three following assumptions: (i) We assume that not only the length L of the rod is fixed but so is the number of the grains N within the beam path. It is reasonable to make this assumption if the ratios satisfy

$$\frac{\sigma_l}{\langle l_g\rangle} \ll \frac{1}{\sqrt{N}}, \quad (13)$$

which means that the average deviation in the number of the grains is much less than unity, and, consequently, the number of grains may be treated as a constant. (ii) The orientation of crystallographic axes in a certain grain is assumed to be independent of the neighboring grains. (iii) The distribution function for a single grain $f(l_g, \alpha, \beta, \Phi)$ is assumed to be uniform with respect to the angular part and to be Gaussian with respect to l_g (see Section 3), where l_g, α, β, and Φ are independent random variables. Therefore, according to assumption (ii), the total distribution function for the whole sample is

$$F[(l_g, \alpha, \beta, \Phi)_1, (l_g, \alpha, \beta, \Phi)_2, \ldots, (l_g, \alpha, \beta, \Phi)_N] = \prod_{i=1}^{N} f[(l_g, \alpha, \beta, \Phi)_i], \quad (14)$$

where i is a grain's number.

Below, we describe the method of averaging the expressions in Eqs. (8a)–(8e). This procedure is significantly simplified by application of the quaternion formalism[9,17] instead of the traditional Jones matrix formalism. According to the quaternion approach, each grain is described by a normalized quaternion (a hypercomplex number of unit norm).

First we describe the transition from the Jones matrix formalism to the quaternion formalism. Every optical element is related to some unitary Jones matrix $\mathbf{U}$:

$$\mathbf{U}\mathbf{U}^* = \boldsymbol{\sigma}_0 = \begin{bmatrix} 1 & 0 \\ 0 & 1 \end{bmatrix}, \quad (15)$$

We write an arbitrary unitary matrix $\mathbf{U}$ as

$$\mathbf{U} = \begin{bmatrix} \alpha_0 + i\alpha_1 & \alpha_2 + i\alpha_3 \\ -\alpha_2 + i\alpha_3 & \alpha_0 - i\alpha_1 \end{bmatrix}, \quad (16)$$

where $|\alpha_0|^2 + |\alpha_1|^2 + |\alpha_2|^2 + |\alpha_3|^2 = 1$. Equation (16) can be expressed in terms of Pauli matrices σ_i, where

$$\boldsymbol{\sigma}_1 = \begin{bmatrix} i & 0 \\ 0 & -i \end{bmatrix}, \qquad \boldsymbol{\sigma}_2 = \begin{bmatrix} 0 & 1 \\ -1 & 0 \end{bmatrix}, \qquad \boldsymbol{\sigma}_3 = \begin{bmatrix} 0 & i \\ i & 0 \end{bmatrix}$$

as

$$\mathbf{U} = \alpha_0\sigma_0 + \alpha_1\sigma_1 + \alpha_2\sigma_2 + \alpha_3\sigma_3. \quad (17)$$

Matrices σ_i ($i = 1, 2, 3$) satisfy the following conditions:

$$\sigma_i^2 = -\sigma_0, \qquad \sigma_i\sigma_j = -\sigma_i\sigma_j = \sigma_k, \quad (18a)$$

where i, j, k are cyclic permutations of the subscripts 1, 2, 3.

The algebra of 2×2 complex matrices is isomorphic to the algebra of quaternions, which are hypercomplex numbers with three imaginary units, I, J, and K, that satisfy relations analogous to Eqs. (18a):

$$I^2 = J^2 = K^2 = -1, \quad IJ = -JI = K,$$
$$JK = -KJ = I, \qquad KI = -IK = J. \quad (18b)$$

Thus we make the following changes of variables:

$$\sigma_0 \to 1, \qquad \sigma_1 \to I, \qquad \sigma_2 \to J, \qquad \sigma_3 \to K, \quad (19)$$

and treat matrix $\mathbf{U}$ as a quaternion, $U = \alpha_0 + \alpha_1 I + \alpha_2 J + \alpha_3 K$.

For each quaternion U there is a conjugate $U^* = \bar{\alpha}_0 - \bar{\alpha}_1 I - \bar{\alpha}_2 J - \bar{\alpha}_3 K$ and a norm $UU^* = U^*U = |\alpha_0|^2 + |\alpha_1|^2 + |\alpha_2|^2 + |\alpha_3|^2$. Unitary matrices are described by quaternions of the unit norm.

We define quaternion $\langle G_0\rangle$ that corresponds to matrix $\langle \mathbf{G}_0\rangle$. Factorable distribution function (14) allows us to perform the consecutive averaging of the expressions in Eqs. (8a)–(8e):

$$\langle G_0\rangle = \langle Q_N{}^*\langle Q_{N-1}{}^*\langle \ldots\langle Q_2{}^*\langle Q_1{}^*MQ_1\rangle|_1 Q_2\rangle|_2 \ldots\rangle|_{N-2} \times Q_{N-1}\rangle|_{N-1}Q_N\rangle|_N,$$

where

$$M = [1 + iI\cos(2\varphi) - iK\sin(2\varphi)]/2,$$

$$Q_k = Q(\delta_{lk}, \delta_{ck}, \theta_k) = \cos(\delta_k/2) + I\sin(\delta_k/2)\cos(2\theta_k)\delta_{lk}/\delta_k - J\sin(\delta_k/2)\delta_{ck}/\delta_k - K\sin(\delta_k/2)\sin(2\theta_k)\delta_{lk}/\delta_k, \quad (20)$$

and $\langle \ldots\rangle|_k$ denotes the average over the kth set of variables:

$$\langle \ldots\rangle|_k \equiv \int_0^\infty \mathrm{d}(l_g)_k \int_{-\pi}^{\pi} \mathrm{d}\alpha_k \int_{-\pi/2}^{\pi/2} \mathrm{d}\beta_k \int_{-\pi}^{\pi} \mathrm{d}\Phi_k \{(\ldots) \times f[(l_g)_k, \alpha_k, \beta_k, \Phi_k]\}. \quad (21)$$

For the quaternion $G_0{}^k \equiv Q_k{}^*\ldots Q_2{}^*Q_1{}^*MQ_1Q_2\ldots Q_k = x_k + Iy_k + Jz_k + Kw_k$, left and right multiplication by Q_{k+1} and Q_{k+1}^*, respectively, yields the transformation of the real and imaginary parts, $G_0^{k+1} = x_{k+1} + Iy_{k+1} + Jz_{k+1} + Kw_{k+1}$, that can be written as

$$x_{k+1} = x_k,$$
$$\begin{pmatrix} y_{k+1} \\ z_{k+1} \\ w_{k+1} \end{pmatrix} = \mathbf{S}(X_{k+1}, Y_{k+1}, Z_{k+1}, W_{k+1}) \begin{pmatrix} y_k \\ z_k \\ w_k \end{pmatrix}, \quad (22)$$

where X, Y, Z, W are the components of the quaternion Q, i.e., $Q_{k+1} = X_{k+1} + IY_{k+1} + JZ_{k+1} + KW_{k+1}$, and where $x_0 = 1/2, y_0 = i\cos(2\varphi)/2, z_0 = 0, w_0 = -i\sin(2\varphi)/2$, and

$$\mathbf{S}(X, Y, Z, W) = \begin{bmatrix} X^2 + Y^2 - Z^2 - W^2 & 2(YZ + XW) & 2(YW - XZ) \\ 2(YX - XW) & X^2 - Y^2 + Z^2 - W^2 & 2(ZW + XY) \\ 2(YW + XZ) & 2(ZW - XY) & X^2 - Y^2 - Z^2 + W^2 \end{bmatrix}.$$

As the $\mathbf{S}$ matrix and distribution function F have an equivalent form for each grain, every step of averaging in Eqs. (20) reduces to multiplication of vector (y_k, z_k, w_k) by the same matrix $\langle \mathbf{S}\rangle$, which is a matrix that comprises the corresponding average (over l_g, α, β, and Φ) elements of the $\mathbf{S}$ matrix. Thus, to find the total quaternion (matrix) $\langle \mathbf{G}_0\rangle$, one needs to raise $\langle \mathbf{S}\rangle$ to the Nth power. Therefore the depolarization, Eq. (7), is determined by matrix $\mathbf{S}_t = \langle \mathbf{S}\rangle^N$.

Note that every optical element that is being described by a normalized quaternion can be related to a unitary 3×3 matrix $\mathbf{S}$, which assigns a transformation like that of Eq. (22). If matrix $\mathbf{U}$ is not unitary, this transformation is determined by a 4×4 matrix [as long as $\mathrm{Re}(G^{k+1}) \neq \mathrm{Re}(G^k)$].

We remark on one more important property of $\mathbf{S}$ matrices. By construction, the matrix associated with the product of two Jones matrices, $\mathbf{U} = \mathbf{U}_1\mathbf{U}_2$, is matrix $\mathbf{S} = \mathbf{S}_1\mathbf{S}_2$, equal to the product of the corresponding $\mathbf{S}$ matrices. Therefore, to find the $\mathbf{S}$ matrix for some optical system, one has to multiply sequentially the $\mathbf{S}$ matrices of the individual elements of the system.

Using the prescribed properties, we can compute the depolarization ratio for all the designs in Fig. 1. A Faraday element is described by the following $\mathbf{S}$ matrix:

$$\mathbf{S}(\delta_l, \delta_c, \theta) = 1 + \sin\delta \begin{bmatrix} -\tan(\delta/2)[1 - (\delta_l/\delta)^2 \cos^2(2\theta)] & -(\delta_l/\delta)\sin(2\theta)[1 + (\delta_c/\delta)\tan(\delta/2)\cot(2\theta)] \\ (\delta_l/\delta)\sin(2\theta)[1 - (\delta_c/\delta)\tan(\delta/2)\cot(2\theta)] & -(\delta_l/\delta)^2 \tan(\delta/2) \\ -(\delta_c/\delta) - (\delta_l/\delta)^2 \tan(\delta/2)\sin(4\theta) & -(\delta_l/\delta)\cos(2\theta)[1 - (\delta_c/\delta)\tan(\delta/2)\tan(2\theta)] \end{bmatrix}$$

$$\begin{bmatrix} (\delta_c/\delta) - (\delta_l/\delta)^2 \tan(\delta/2)\sin(4\theta) \\ \times (\delta_l/\delta)\cos(2\theta)[1 + (\delta_c/\delta)\tan(\delta/2)\tan(2\theta)] \\ -\tan(\delta/2)[1 - (\delta_l/\delta)^2 \sin^2(2\theta)] \end{bmatrix}. \tag{23}$$

All further derivations are merely from perturbation theory with a small parameter $\varepsilon = p/N$, which is the unitless power deposited in one grain. As the heat released in FEs is relatively small, we assume that $\Delta_l = pa \ll \Delta_c \sim \pi/2$, and we keep the terms up to second order $(\Delta_l)^2$ $(\sim p^2)$ in expressions proportional to $1/N$. Taking the average of Eq. (23) and raising it to the Nth power, we obtain

$$\langle\Gamma_c\rangle = \frac{\Delta_l^4}{4\Delta_c^4}(\Delta_c - \sin\Delta_c)^2 + \frac{p^2}{8N}(A + B), \tag{25c}$$

$$\langle\Gamma_d\rangle = \frac{p^2}{8N}(A + B), \tag{25d}$$

$$\mathbf{S}_t = \begin{bmatrix} (1/\Delta^2)(\Delta_l^2 + \Delta_c^2 \cos\Delta) & (\Delta_l\Delta_c/\Delta^2)(1 - \cos\Delta) & (\Delta_c/\Delta)\sin\Delta \\ (\Delta_l\Delta_c/\Delta^2)(1 - \cos\Delta) & (1/\Delta^2)(\Delta_c^2 + \Delta_l^2 \cos\Delta) & -(\Delta_l/\Delta)\sin\Delta \\ -(\Delta_c/\Delta)\sin\Delta & (\Delta_l/\Delta)\sin\Delta & \cos\Delta \end{bmatrix} - \frac{p^2}{4N}\mathbf{S}_1,$$

where

$$\mathbf{S}_1 = \begin{bmatrix} (A + B)\cos\Delta + (B - A)(\sin\Delta/\Delta) & 0 & (A + B)\sin\Delta \\ 0 & 2(A + B) & 0 \\ -(A + B)\sin\Delta & 0 & (A + B)\cos\Delta - (B - A)(\sin\Delta/\Delta) \end{bmatrix},$$

$$\Delta^2 = \Delta_l^2 + \Delta_c^2, \quad \Delta_l = pa, \quad a = \langle\tilde{a}\rangle = Xh, \quad X = \frac{75\xi + 53}{128},$$

$$A = \langle\tilde{a}^2\rangle - a^2 = (1 + d^2)(h^2/2^{16})(22665\xi^2 + 31470\xi + 11401) + B - (Xh)^2,$$

$$B = \langle\tilde{b}^2\rangle = (1 + d^2)\frac{(\xi - 1)^2}{2^{17}}(1060g^2 + 9865h^2), \quad d = \frac{\sigma_l}{\langle l_g\rangle}. \tag{24}$$

The quantity of greater interest is not the local depolarization but rather the integral depolarization, which characterizes the isolation ratio of Faraday isolators. Below we introduce the local depolarization averaged over φ, $\langle\Gamma\rangle$, and integral depolarization γ as a function of the heat power released, p (for a TGG crystal with constant $\xi = 2.25$ and $X = 1.73$):

$$\langle\Gamma_a\rangle = (1 - \cos\Delta_c)\frac{\Delta_l^2}{4\Delta_c^2} + \frac{p^2}{8N}(A + B), \tag{25a}$$

$$\langle\Gamma_b\rangle = \frac{\Delta_l^4}{\Delta_c^2}\left[\frac{\sin^2(\Delta_c/2)}{2} + \frac{(\sin\Delta_c - \Delta_c)^2}{\Delta_c^2}\right] + \frac{p^2}{8N}(A + B), \tag{25b}$$

$$\langle\Gamma_e\rangle = (1 - \cos\Delta_c)\frac{\Delta_l^2}{4\Delta_c^2} + \frac{p^2}{8N}(A + B), \tag{25e}$$

$$\langle\Gamma_f\rangle = \frac{9}{16}\frac{\Delta_l^4}{\Delta_c^4}\left(\Delta_c - \frac{1}{\sin\Delta_c}\right)^2 + \frac{p^2}{8N}(A + B). \tag{25f}$$

Let us discuss the optimal beam shape. As distinct from, say, laser active elements, in which it is worthwhile to maintain wide flat-shaped beams to convert all the energy stored in population inversion, there is no such requirement in the case of Faraday devices. In dealing with a Faraday device one is free to choose the ratio of sample radius R_0 to the radius of the (Gaussian) beam, r_0. On the one hand, the Faraday device has to be large enough to prevent beam cutoff. On the other hand, the ability to produce large samples as well to maintain a

magnetic field within them are limited. Thus, for any type of magneto-optical medium the optimal ratio R_0/r_0 is 2–4. Below for comparison we write the formulas for the integral depolarization that corresponds to flat-shaped and Gaussian [for $R = (R_0/r_0)^2 = 10$] beams:

$$\gamma_a^{\text{flat}} = 0.00634p^2 + 0.00275(p^2/N),$$
$$\gamma_a^{\text{Gauss}} = 0.01043p^2 + 0.00933(p^2/N), \quad (26a)$$

$$\gamma_b^{\text{flat}} = 0.00023p^4 + 0.00275(p^2/N),$$
$$\gamma_b^{\text{Gauss}} = 0.00076p^4 + 0.00933(p^2/N), \quad (26b)$$

$$\gamma_c^{\text{flat}} = 0.00003p^4 + 0.00275(p^2/N),$$
$$\gamma_c^{\text{Gauss}} = 0.00152p^2 + 0.00933(p^2/N), \quad (26c)$$

$$\gamma_d^{\text{flat}} = 0.00275(p^2/N),$$
$$\gamma_d^{\text{Gauss}} = 0.00091p^2 + 0.00933(p^2/N), \quad (26d)$$

$$\gamma_e^{\text{flat}} = 0.00317p^2 + 0.00550(p^2/N),$$
$$\gamma_e^{\text{Gauss}} = 0.0209p^2 + 0.01866(p^2/N), \quad (26e)$$

$$\gamma_f^{\text{flat}} = 0.00004p^4 + 0.00550(p^2/N),$$
$$\gamma_f^{\text{Gauss}} = 0.00013p^4 + 0.01866(p^2/N). \quad (26f)$$

5. Results and Discussion

It is easy to show that, in the limit $N \to \infty$, Eqs. (25) and (26) for Γ_{a-f} and γ_{a-f} practically coincide with the corresponding expressions[15,20–23] for a single crystal with orientation [111]. The only difference is that in characteristic quantity X. Specifically, for a single crystal $X = (1 + 2\xi)/3$, whereas for ceramics $X = (75\xi + 53)/128$. In other words, when $N \to \infty$, ceramics are equivalent to a single [111] crystal whose effective constant ξ_{eff} is defined as

$$\xi_{\text{eff}} - 1 = (\xi - 1)(15/16)^2. \quad (27)$$

The physical meaning of the effective constant is that a ceramic sample with constant ξ has the same polarization properties as a [111]-oriented single crystal with constant ξ_{eff}. For TGG in particular, $\xi = 2.25$ and $\xi_{\text{eff}} = 1.78$, which lead to a minor difference in the integral depolarization.

In Fig. 3 analytical curves of $\gamma(p)$ [Eqs. (25)] for TGG ceramics that correspond to different designs are shown. At finite values of N, Eqs. (26) are obtained as the result of a Taylor series expansion in the small parameter $\varepsilon = p/N$ if terms of order ε^2 are neglected. The additional (with respect to $N = \infty$) depolarization is proportional to the quantity p^2N^{-1} and is due to the presence of mean-square deviation D_Γ. Applying an approach analogous to that which was used above, one can verify that

$$D_\Gamma = (\langle\Gamma^2\rangle - \langle\Gamma\rangle^2) \sim p^2/N, \quad (28)$$

which is also in agreement with numerical results[7] and constitutes an important consequence of the random nature of thermally induced birefringence in ceramics. Indeed, consider an optical system consisting of m se-

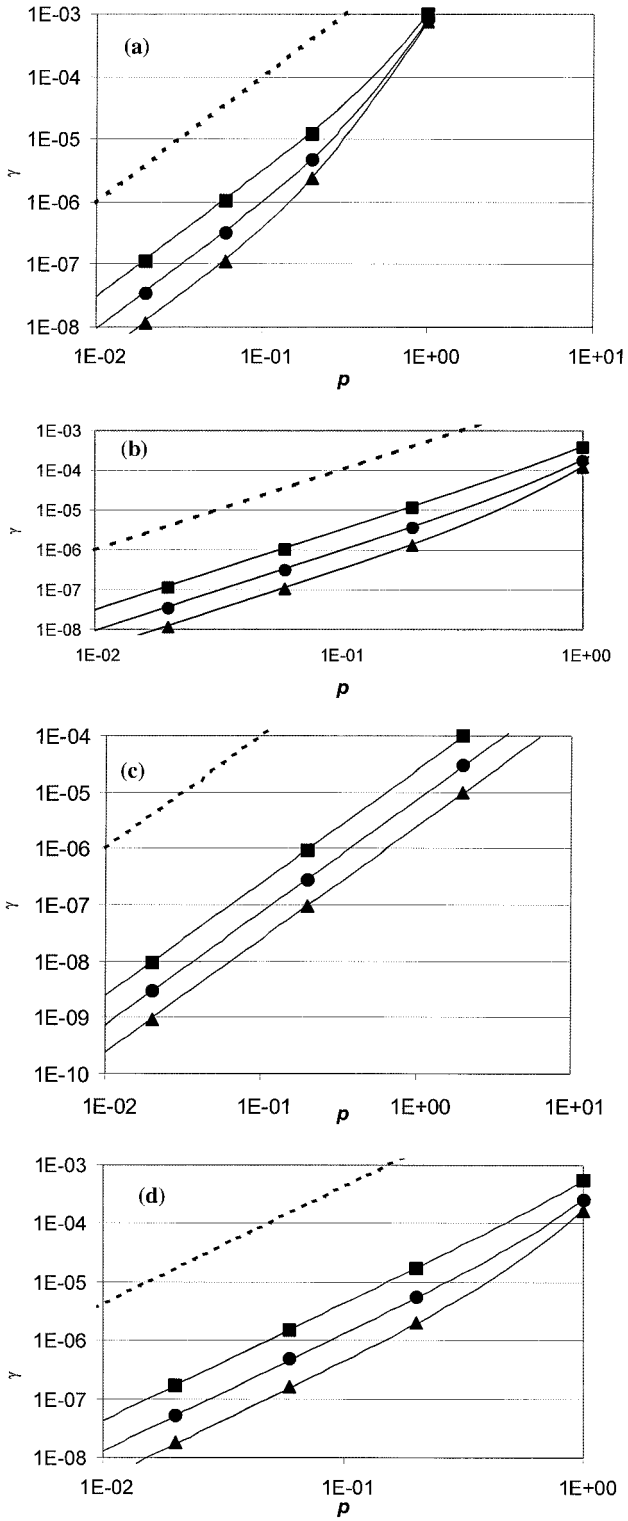

Fig. 3. Dependence of γ on p Faraday isolators and mirrors made from TGG ceramics for $N = 30$ (squares), $N = 100$ (circles), and $N = 300$ (triangles): (a) on the design of the Faraday isolator shown in Fig. 1(b), (b) on the design of the Faraday isolator shown in Fig. 1(c), (c) on the design of the Faraday isolator shown in Fig. 1(d), and (d) on the design of the Faraday mirror shown in Fig. 1(f). Dashed curves in (a)–(c) show the dependence on the design of the Faraday isolator without compensation shown in Fig. 1(a), and the dashed curve in (d) shows the dependence on the design of the Faraday mirror without compensation shown in Fig. 1(e).

quential ceramic samples, each of which is characterized by a number of grains N_0 and by the heat power released, p_0. In this case, one can treat the system as one sample that comprises $N = mN_0$ grains with total deposited power $p = mp_0$. Then, according to relation (28), the mean-square deviation of the local depolarization in this optical system, D_Γ, is m times greater than that in each individual sample, $D_{\Gamma 0}$; i.e., $D_\Gamma = mD_{\Gamma 0}$. The latter result resembles the classic random-walk problem, wherein the mean-square displacement is proportional to the number of steps.

This phenomenon becomes transparent when the linear birefringence is sufficiently weak, i.e., $\Delta_l \ll \pi/2$. Thus in Eqs. (25) the quantity

$$\frac{p^2}{N}(A + B) = D[\Delta_l] = \frac{p^2}{N}(\xi - 1)^2 \frac{5}{2^{11}}(106g^2 + 1003h^2), \tag{29}$$

which determines corrections of order $\sim 1/N$, is nothing else but the variation of thermally induced phase delay Δ_l. The second term in each of Eqs. (25) and (26) is in accord with this:

$$\gamma_a = \gamma_b = \gamma_c = \gamma_d = \gamma_e/2 = \gamma_f/2.$$

In the last two designs, the laser beam travels a round trip, such that effectively the number of ceramic samples doubles. In other words, if we normalized power p and number of grains N such that they would mean the total power and that total number of grains (for the entire beam path), the corrections to the depolarization in all the designs would be identical.

Two laser beams spaced by the grain size in a transverse direction pass through independent sets of grains. Therefore the depolarization that corresponds to these beams will be different. Thus the large-scale structure of the outgoing radiation will have superimposed upon it an intensity modulation with characteristic scale $\langle l_g \rangle$. This modulation is caused by the dispersion of depolarization D_Γ, and its depth grows with the increase in p^2/N. The presence of different grains within two adjacent beams' paths may cause not only amplitude modulation of the transmitted wave but phase modulation as well.

Now it is pertinent to discuss the validity of the geometrical approach that we have used. The mean grain size is much less than the characteristic scale of the temperature gradient governing the change in the index of refraction. As the distance between any adjacent grains is much less than the wavelength, we may assume that the beam will remain parallel to the axis of the rod while it is traveling through the sample. In Ref. 29 a formula for the mean-square lateral displacement of a light beam propagating in randomly inhomogeneous media was derived. As applied to ceramics, this formula shows the beam's lateral displacement to be of the order of $\rho = 0.1N^{1/2}\lambda p$. As a rule, ρ is less than $\langle l_g \rangle$. Otherwise, the characteristic scale of the aforementioned modulation will be equal to ρ rather than to $\langle l_g \rangle$.

It is necessary to mention that the numerical results (the dashed curves in Fig. 3) are obtained by simulation of a slightly different, more physical problem—assuming that only the length of the FE is fixed, whereas the number of grains within a beam path is allowed to be a random variable. These two statements of the problem are completely equivalent if we set the length of a grain to be constant, that is, tantamount to the condition $d = \sigma_l/\langle l_g \rangle = 0$. The curves in Fig. 3 are plotted exactly for this case. The validity of the comparison of the results for the two given problems is reasonably held if $d < 1/N^{1/2}$ (inequality (13)], which means that the average deviation in the number of the grains is much less than unity, and, consequently, the number of grains may be treated as constant. Note that the numerical calculations[7] have shown a small dependence of the depolarization on d.

Let us now discuss the possibility of defining a Jones matrix for ceramic samples. Throughout the solution we were using $\mathbf{S}$ matrices, which do have direct physical meaning. However, if some 3×3 matrix can be cast in the form of Eq. (23), then it is possible to relate a quaternion and, hence, a Jones matrix to it. In particular, if we neglect the terms of order $1/N$ in the expression for $\mathbf{S}_t$, it is easy to see that ceramics are equivalent to a single crystal. In that case the effective Jones matrix (in the primed Fig. 2 coordinate system) for ceramic FEs is given by $\mathbf{Q}(\Delta_l, \Delta_c, 0)$, from Eq. (5). [$\Delta_l$ is defined by Eqs. (24) and has the meaning of the effective phase delay over the whole ceramic sample.] In other words, one is to take the regular Jones matrix for the FE written in terms of the effective ξ in accord with Eq. (27). Using Eq. (5), one can treat the latter matrix as a regular Jones matrix, i.e., multiply it by matrices related to other optical elements (both usual and ceramic) and get correct expressions for the average depolarization in any optical system.

6. Conclusions

Summing up the ideas discussed above, we draw the following conclusions:

1. With respect to the polarization features, ceramics are fairly similar to a single crystal with [111] orientation if the ratio of the Faraday element's length to the mean grain size is $N \to \infty$. Specifically, the dispersion of the depolarization vanishes, whereas the depolarization itself is described by the corresponding formulas for a [111] single crystal up to the change in the parameter ξ according to Eq. (27).
2. The efficiency of birefringence compensation in ceramics by means of all known techniques is lower than that for a single crystal. The increase in depolarization in ceramics compared with a single crystal is proportional to p^2N^{-1}.
3. Both polarized and depolarized radiation always has small-scale modulation with a characteris-

tic size of approximately the grain size, $\langle l_g \rangle$. This modulation increases with the growth of $p^2 N^{-1}$.

4. Given reasonable values of N ($N \geq 100$), depolarization corrections [proportional to $p^2 N^{-1}$ in Eq. (26)] become comparable with the main terms at $p \leq 0.1$. At such small p, total depolarization is practically negligible. Therefore, corrections concerned with phase-delay variation do not play a substantial role.

5. When thermally induced birefringence is weak ($\Delta_l \ll \pi/2$) it is possible to define an effective Jones matrix to describe a ceramic element according to Eqs. (5) and (27).

The authors gratefully acknowledge support of this research by the National Science Foundation (grant PHY0244902).

References

1. T. Taira, A. Ikesue, and K. Yoshida, "Diode-pumped Nd:YAG ceramics lasers," in *Advanced Solid-State Lasers*, W. Bosenberg and M. M. Fejer, eds., Vol. 19 of OSA Trends in Optics and Photonics Series (Optical Society of America, Washington, D.C., 1998), pp. 430–432.
2. J. Lu, M. Prabhu, J. Song, C. Li, J. Xu, K. Ueda, A. A. Kaminskii, H. Yagi, and T. Yanagitani, "Optical properties and highly efficient laser oscillation of Nd:YAG ceramic," Appl. Phys. B **71,** 469–473 (2000).
3. I. Shoji, S. Kurimura, Y. Sato, T. Taira, A. Ikesue, and K. Yoshida, "Optical properties and laser characteristics of highly Nd^{3+}-doped $Y_3Al_5O_{12}$ ceramics," Appl. Phys. Lett. **77,** 939–941 (2000).
4. J. R. Lu, J. H. Lu, T. Murai, K. Takaichi, T. Uematsu, K. Ueda, H. Yagi, T. Yanagitani, and A. A. Kaminskii, "Nd^{3+}:Y_2O_3 ceramic laser," Jpn. J. Appl. Phys. Part 2 **40,** L1277–L1279 (2001).
5. J. Lu, T. Murai, K. Takaichi, T. Uematsu, K. Misawa, M. Prabhu, J. Xu, K. Ueda, H. Yagi, T. Yanagitani, A. A. Kaminskii, and A. Kudryashov, "72-W Nd:$Y_3Al_5O_{12}$ ceramic laser," Appl. Phys. Lett. **78,** 3586–3588 (2001).
6. I. Shoji, Y. Sato, S. Kurimura, V. Lupei, T. Taira, A. Ikesue, and K. Yoshida, "Thermal-birefringence-induced depolarization in Nd:YAG ceramics," Opt. Lett. **27,** 234–236 (2002).
7. E. A. Khazanov, "Thermally induced birefringence in Nd:YAG ceramics," Opt. Lett. **27,** 716–718 (2002).
8. M. A. Kagan and E. A. Khazanov, "Compensation of thermally induced birefringence in active medium made of polycrystalline ceramics," in *Solid State Lasers XII*, R. Scheps, ed., Proc. SPIE **4968,** 151–162 (2003).
9. M. A. Kagan and E. A. Khazanov, "Features of compensation of thermally induced depolarization in polycrystalline Nd:YAG ceramic," Quantum Electron. **33,** 876–882 (2003).
10. A. Ikesue, I. Furusato, and K. Kamata, "Fabrication of polycrystalline, transparent YAG ceramics by a solid-state reaction method," J. Am. Ceram. Soc. **78,** 225–228 (1995).
11. A. Ikesue, T. Kinoshita, K. Kamata, and K. Yoshida, "Fabrication and optical properties of high-performance polycrystalline Nd:YAG ceramics for solid-state lasers," J. Am. Ceram. Soc. **78,** 1033–1040 (1995).
12. I. Shoji, S. Kurimura, Y. Sato, T. Taira, A. Ikesue, and K. Yoshida, "Optical properties and laser characteristics of highly Nd^{3+}-doped $Y_3Al_5O_{12}$ ceramics," J. Am. Ceram. Soc. **79,** 1921–1941 (1995).
13. K. Takaichi, J. R. Lu, T. Murai, T. Uematsu, A. Shirakawa, K. Ueda, H. Yagi, T. Yanagitani, and A. A. Kaminskii, "Chromium doped $Y_3Al_5O_{12}$ ceramics—a novel saturable absorber for passively self-*Q*-switched one-micron solid state lasers," Jpn. J. Appl. Phys. Part 2 **41,** L96–L98 (2002).
14. A. Ikesue, Japan Fine Ceramics Center, 2-4-1 Mutsuno, Atsuta-ku, Nagoya 456-8587 Japan (personal communication, 2002).
15. E. A. Khazanov, "Compensation of thermally induced polarization distortions in Faraday isolators," Quantum Electron. **29,** 59–64 (1999).
16. E. A. Khazanov, O. V. Kulagin, S. Yoshida, D. Tanner, and D. Reitze, "Investigation of self-induced depolarization of laser radiation in terbium gallium garnet," IEEE J. Quantum Electron. **35,** 1116–1122 (1999).
17. L. Ainola and H. Aben, "Transformation equations in polarization optics of inhomogeneous birefringent media," J. Opt. Soc. Am. A **18,** 2164–2170 (2001).
18. M. J. Tabor and F. S. Chen, "Electromagnetic propagation through materials possessing both Faraday rotation and birefringence: experiments with ytterbium orthoferrite," Appl. Phys. **40,** 2760–2765 (1969).
19. A. P. Voytovich and V. N. Severikov, *Lasers with Anisotropic Resonators* (Nauka, Minsk, 1988).
20. E. Khazanov, N. Andreev, A. Babin, A. Kiselev, O. Palashov, and D. Reitze, "Suppression of self-induced depolarization of high-power laser radiation in glass-based Faraday isolators," J. Opt. Soc. Am. B **17,** 99–102 (2000).
21. N. F. Andreev, E. V. Katin, O. V. Palashov, A. K. Potemkin, D. Reitze, A. M. Sergeev, and E. A. Khazanov, "The use of crystalline quartz for compensation for thermally indused depolarization in Faraday isolators," Quantum Electron. **32,** 91–94 (2002).
22. E. A. Khazanov, "A new Faraday rotator for high average power lasers," Quantum Electronics **31,** 351–356 (2001).
23. E. A. Khazanov, A. A. Anastasiyev, N. F. Andreev, A. Voytovich, and O. V. Palashov, "Compensation of birefringence in active elements with a novel Faraday mirror operating at high average power," Appl. Opt. **41,** 2947–2954 (2002).
24. E. Khazanov, N. Andreev, O. Palashov, A. Poteomkin, A. Sergeev, O. Mehl, and D. Reitze, "Effect of terbium gallium garnet crystal orientation on the isolation ratio of a Faraday isolator at high average power," Appl. Opt. **41,** 483–492 (2002).
25. L. D. Landau and E. M. Lifshits, *Theoretical Physics: Mechanics* (Nauka, Moscow, 1973).
26. A. V. Mezenov, L. N. Soms, and A. I. Stepanov, *Thermooptics of Solid-State Lasers* (Mashinostroenie, Leningrad, USSR, 1986).
27. L. N. Soms and A. A. Tarasov, "Thermal deformation in color-center laser active elements. 1. Theory," Sov. J. Quantum Electron. **9,** 1506–1508 (1979).
28. E. Khazanov, N. Andreev, A. Mal'shakov, O. Palashov, A. Poteomkin, A. Sergeev, A. Shaykin, V. Zelenogorsky, I. Ivanov, R. Amin, G. Mueller, D. B. Tanner, and D. H. Reitze, "Compensation of thermally induced modal distortions in Faraday isolators," IEEE J. Quantum Electron. (to be published).
29. S. M. Ritov, Y. A. Kravtsov, and B. T. Tatarskii, *Introduction to Statistical Radiophysics* (Nauka, Moscow, 1978).